THE JOURNAL OF PHYSICAL CHEMISTRY A
A JOURNAL OF THE AMERICAN CHEMICAL SOCIETY

pubs.acs.org/JPCA Article

Electronic Structures of an Annulated *meso*-Tetraphenylchlorin and a Related Chlorin Analogue Incorporating an 8-Membered Ring through MCD Spectroscopy and DFT Calculations

Dustin E. Nevonen, Adewole O. Atoyebi, Michael P. Luciano, Christian Brückner,* and Victor N. Nemykin*

Cite This: https://doi.org/10.1021/acs.jpca.4c02803 Read Online

ACCESS | Metrics & More | Article Recommendations | Supporting Information

ABSTRACT: Herein, we compare the electronic structures of the metal-free and nickel(II) derivatives of an annulated *meso*-tetraphenyldihydroxychlorin with those of the (metallo)chlorin analogues derived by pyrroline β,β'-ring cleavage of the annulated (metallo)chlorins. These (metallo)chlorin analogues incorporate 8-membered heterocycles in place of the pyrroline, carry oxo-functionalities on the former pyrroline β-carbon atoms, and were previously shown to possess drastically ruffled (twisted) nonplanar conformations. The magnetic circular dichroism spectra of all chromophores investigated feature chlorin-like UV−vis spectra and correspondingly reversed (positive-to-negative in ascending energy) sign sequences in the Q-band region, indicative of ΔHOMO < ΔLUMO relationships. Density functional theory (DFT) calculations indicate that the HOMOs in all compounds are a_{1u}-type molecular orbitals (in traditional for the porphyrin spectroscopy D_{4h} point group). Time-dependent DFT calculations correlate well with the experimental spectra and indicate that Gouterman's four-orbital model can be applied to these chromophores. This work highlights to which degree synthetic chlorin analogues can deviate from the structural parameters of natural chlorins without losing their electronic chlorin characteristics.

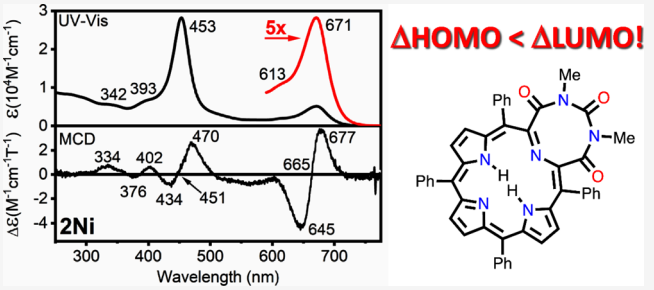

INTRODUCTION

Porphyrins and hydroporphyrins, members of the "pigments of life",[1] are 18 π-electron tetrapyrrolic macrocycles which can either be synthetically prepared or isolated from natural sources.[2−7] Reduction of a single peripheral pyrrolic double bond of a porphyrin generates chlorins; this modification results in dramatic changes in the electronic structure and UV−vis absorption profile of the chromophore.[5,8,9] The diagnostic features of the optical spectra of the porphyrins and hydroporphyrins originate from electronic transitions between the frontier orbitals.[10,11]

Magnetic circular dichroism (MCD) spectroscopy provides a unique opportunity to directly probe the energy gaps between frontier occupied and unoccupied orbitals of porphyrinoids.[12−16] Typically, naturally occurring β-alkyl porphyrins show a ΔHOMO > ΔLUMO relationship, whereby ΔHOMO is the energy difference between Gouterman's a_{1u}-type and a_{2u}-type molecular orbitals (MOs) in traditional for porphyrin spectroscopy D_{4h} point group notation,[10,11] and ΔLUMO is the energy difference between $e_{g(x)}$-type and $e_{g(y)}$-type MOs. Hydroporphyrins, such as chlorins, have a reversed ΔHOMO < ΔLUMO relationship. Following Michl's perimeter model,[12,17] the ΔHOMO > ΔLUMO relationship is reflected in their MCD spectra by exhibiting a negative-to-positive (in ascending energy) sign sequence in the Q-band region, while the opposite is expected in the MCD spectra of porphyrinoids with a ΔHOMO < ΔLUMO relationship.[12,13,18−26] Typically, these relative and absolute energies of the molecular orbitals of porphyrinoids can also be confirmed by DFT calculations.[16,22−26]

We recently reported the formation of the *N,N'*-dimethylurea adducts to *meso*-tetraphenyl-2,3-dioxochlorin and its nickel complex, generating diol adducts **1** and **1Ni**, respectively (Figure 1).[27,28] The optical properties of the 2,3-dioxochlorin and its nickel complex are much distorted from those of regular chlorins.[29,30] This is expected as there are many examples in the literature that demonstrated the impact of the β-oxo groups on the electronic structure of porphyrins and hydroporphyrins.[23,31−35] On the other hand, the products of $\beta-\beta'$ bond cleavage **2** and **2Ni** possess typical (metallo)chlorin spectra, comparable to those of (metallo)diolchlorins in the absence of the annulated imidazolidinone rings.[28] Correspondingly, the

Received: April 29, 2024
Revised: May 24, 2024
Accepted: May 28, 2024

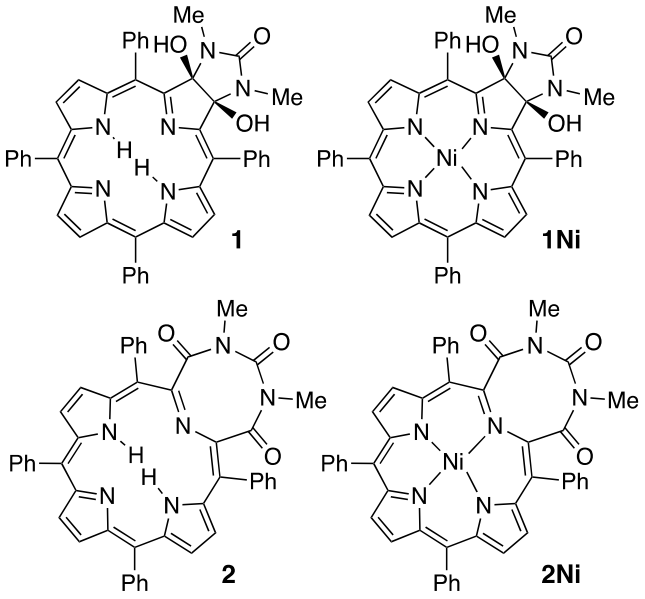

Figure 1. Structures of the free-base (**1**, **2**) and nickel-complexed (**1Ni**, **2Ni**) annulated (**1**, **1Ni**) and pyrrole-expanded chlorins (**2**, **2Ni**).

modest out-of-plane conformations of both chromophores are also qualitatively similar and that of the adduct only slightly more pronounced.[28]

We previously used the diol functionality of *meso*-tetraaryldiolchlorins as a synthetic handle to induce pyrroline β,β'-bond cleavages.[36−38] Applying this methodology to the annulated diols **1** and **1Ni** also cleaved the β,β'-bond, combined the atoms of the annulated ring and the pyrroline, and generated the pyrrole-modified systems **2** and **2Ni**, respectively, containing 8-membered 1,3,6-triazocine-2,4,8-trione rings.[28] The presence of this large heterocycle forces the macrocycles into drastically nonplanar conformations; the oxidative cleavage also introduced two oxo-functionalities on the former β-carbon atoms of the pyrroline. Both structural factors are reflected in the much red-shifted and broadened optical spectra of these "supersized" porphyrins.[28]

In this report, the electronic structures of derivatives **1** and **2** and their corresponding nickel complexes **1Ni** and **2Ni** are investigated using UV−vis and MCD spectroscopy as well as density functional theory (DFT) and time-dependent DFT (TDDFT) with the aim to better define their electronic structures. In particular, the main question we tried to address in this work is how different are the electronic structures of the *seco*-porphyrin-types compounds **2** and **2Ni** from those in chlorin-type compounds **1** and **1Ni.** This study shows that these chromophores, irrespective of their drastic perturbations from regular chlorins, possess the "natural" electronic structure configuration expected for chlorins.

METHODS

Materials. Compounds **1**/**1Ni** and **2**/**2Ni** were synthesized, as described in the literature.[28]

UV−Vis/MCD Spectroscopy. All UV−vis spectra were collected on a Jasco V-770 spectrophotometer, and MCD spectra were measured with a Jasco J-1500 CD spectrophotometer using a Jasco MCD-581 electromagnet operated at 1.0 T. The MCD spectra were recorded as millidegrees $[\theta]$ and converted to molar ellipticity as $\Delta\varepsilon = \theta/(32980 \times Blc)$, where B is the magnetic field, l is the path length (in cm), and c is the concentration (in M). The completed MCD spectra were measured at 10 °C in parallel and antiparallel orientations with respect to the magnetic field.

Computational Aspects. All calculations were run using Gaussian 16.[39] The starting geometries of all compounds were optimized using the M06[40] exchange correlation functional with the full-electron basis set[41] (Ni) and 6-311G(d) basis set[42] for all other atoms. Vibrational frequencies were calculated to ensure that all geometries were local minima. TDDFT with M06 was used to calculate the first 40 excited states for each compound. All calculations were run in solution using the PCM model[43] with dichloromethane as the solvent.

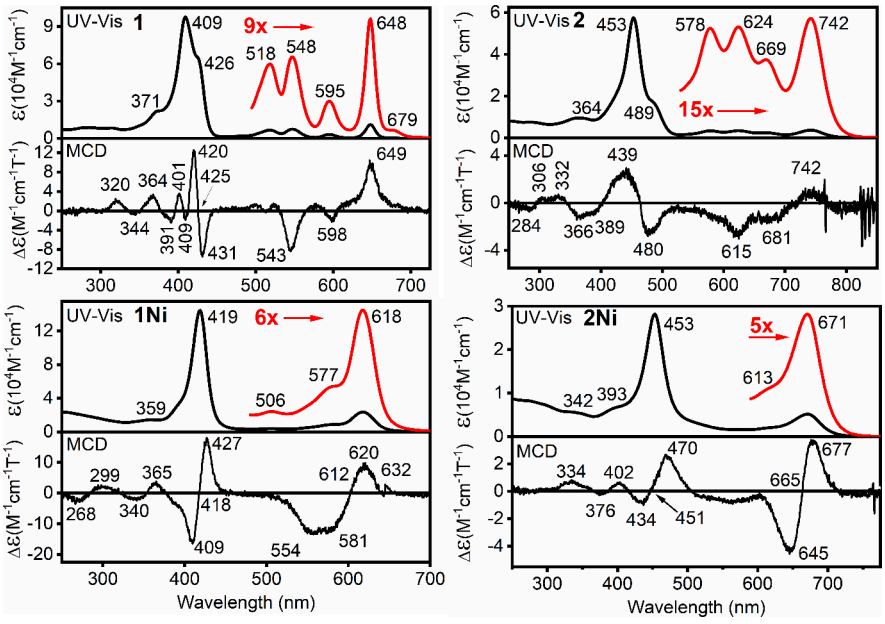

Figure 2. Experimental UV−vis (upper) and MCD (lower) spectra of the compounds indicated (in CH_2Cl_2).

https://doi.org/10.1021/acs.jpca.4c02803
J. Phys. Chem. A XXXX, XXX, XXX−XXX

QMForge[44] was used for the molecular orbital composition analyses and TDDFT band assignments.

RESULTS AND DISCUSSION

The UV−vis and MCD spectra of all of the compounds investigated are shown in Figure 2. Both free-base chromophores **1** and **2** possess chlorin-type UV−vis spectra with a split Soret band and a *Q*-band with associated vibronic satellites, but the spectrum of **2** is significantly red-shifted with a pronounced broadening of all bands.

The UV−vis spectra of **1Ni** and **2Ni** largely resemble those of classic metallochlorins where a dominant Soret band (∼420−455 nm) and smaller *Q*-bands (∼620−670 nm) are defining their spectra.[11] It is clear to see that the systems **2** and **2Ni** with an 8-membered heterocycle have significantly red-shifted Soret and *Q*-bands. In general, the molar absorptivity coefficients of **1** and **1Ni** are substantially higher than those of **2** and **2Ni**, a factor attributed to the drastic nonplanarity of the "supersized" chromophores.[28] The modification of a single pyrrole ring in porphyrins leads to the loss of either D_{2h} (free-base) or D_{4h} (nickel complex) symmetry of the parent chromophore. Thus, in compounds **1**/**1Ni** and **2**/**2Ni**, the observation of the Q_x and Q_y and split Soret bands is expected. Interestingly, elimination of the $\beta-\beta'$ bond in **2** and **2Ni** results in a significant decrease of the molar extinction coefficients in these systems. Such a decrease can be reflective of the nonplanarity increase in these compounds compared to more planar **1** and **1Ni**.

All of these bands should be associated with Faraday *B*-terms in their respective MCD spectra.[13−15] Indeed, the lowest energy transition observed in the UV−vis spectrum of **1** at 648 nm is associated with a *B*-term of the positive amplitude in the corresponding MCD spectrum, and thus, this transition was assigned to the Q_x-band; correspondingly, the lowest energy *B*-term of the negative amplitude observed at 598 nm was assigned as the Q_y-band, and the *B*-term of the negative amplitude observed at 543 nm was assigned as the $Q_y(0-1)$ vibronic satellite. Observed in the UV−vis spectrum of **1**, the lower energy of the split Soret bands (426 nm) is associated with a pseudo MCD *A*-term centered at 425 nm, while the higher-energy Soret band (409 nm) is accompanied by the MCD *B*-terms observed at 409 and 401 nm. Introduction of the nickel ion into free-base **1** (generating compound **1Ni**) does not significantly change the MCD profile in the *Q*-band region. Thus, an MCD *B*-term with the positive amplitude was observed around 740 nm and was assigned as the Q_x-band. Two clear MCD *B*-terms with the negative amplitude observed at 681 and 615 nm were assigned as $Q_y(0-0)$ and $Q_y(0-1)$ transitions, respectively.

In the case of macrocycle compound **1Ni**, the MCD *B*-term with a positive amplitude observed at 620 nm correlates well with the low-energy band observed at 618 nm in the UV−vis spectrum of this compound and was assigned as the Q_x-band. The MCD *B*-term of the negative amplitude observed at 581 nm correlates with the 577 nm band in the UV−vis spectrum and was assigned as the $Q_y(0-0)$ transition. Another *B*-term observed at 554 nm has no visible counterpart in the UV−vis spectrum of **1Ni** and was assigned as the $Q_y(0-1)$ transition. Contrary to the MCD spectra of **1**/**1Ni** and **2**, a clear pseudo *A*-term centered at 665 nm for **2Ni** correlates with the absorption band at 671 nm and consists of overlapping Q_x and Q_y transitions. Interestingly, metalation of both **1** and **2** results in the inverted MCD pattern in the Soret-band region (Figure 2).

More importantly, in all four compounds, the Q_x/Q_y sequence has a +/− sign sequence for the MCD *B*-terms and is thus, according to Michl's perimeter theory,[12−16,45] suggestive of the characteristic (for chlorins) ΔHOMO < ΔLUMO relationship. This relationship is reflective of a significantly larger perturbation of the initial e_g-type (in a standard D_{4h} symmetry Gouterman's model)[11] LUMO/LUMO+1 set of the orbitals than the a_{1u}/a_{2u}-type HOMO/HOMO−1 pair.

To gain a deeper understanding of the nature and origins of the spectroscopic features as well as the electronic structures of the pyrrole-modified porphyrins **1**/**1Ni** and **2**/**2Ni**, DFT and TDDFT calculations were employed. Shown in Figure 3 are

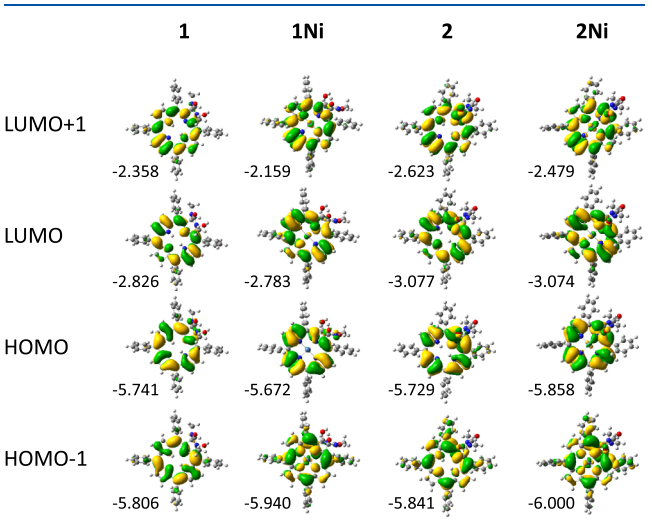

Figure 3. Select DFT-predicted frontier molecular orbitals for the compounds are indicated. Energy values are in eV.

the frontier MOs involved in the major excitations of the Soret and *Q* bands for **1**/**1Ni** and **2**/**2Ni**, while the extended list of MOs is presented in Tables S1−S4. These frontier MOs closely resemble the classical Gouterman's four orbitals for porphyrins.[11] In each case, LUMO and LUMO+1 are representative of Gouterman's doubly degenerate $e_{g(x)}$- and $e_{g(y)}$-type orbitals. Typically, the HOMO of *meso*-tetraphenylporphyrins resembles a Gouterman's a_{2u}-type orbital, and the HOMO−1 is represented by Gouterman's a_{1u}-type orbital; however, according to our DFT calculations, these two orbitals are inverted in energy, and **1**/**1Ni** and **2**/**2Ni** possess an a_{1u}-type HOMO and an a_{2u}-type HOMO−1, respectively. The a_{1u}/a_{2u}-type energy gap in **1** and **2** is significantly smaller than that observed in **1Ni** and **2Ni**. A small separation between Gouterman's a_{1u}-type and a_{2u}-type MOs is quite typical for the synthetic and natural porphyrins.[10−16] This is reflective of the influence of the modified pyrrole fragment on the electronic structure of the porphyrinoids. MO percent composition diagrams are shown in Figure S1 and presented in numerical format in Tables S5−S8.

The DFT-predicted energy-level diagram for **1**/**1Ni** and **2**/**2Ni** presented in Figure 4 clearly shows that the frontier orbitals that are involved in the bulk of photoexcitations (HOMO−1 to LUMO+1) are energetically well-separated from the surrounding orbitals. Furthermore, in each case, ΔHOMO < ΔLUMO. This is specifically the electronic

https://doi.org/10.1021/acs.jpca.4c02803
J. Phys. Chem. A XXXX, XXX, XXX−XXX

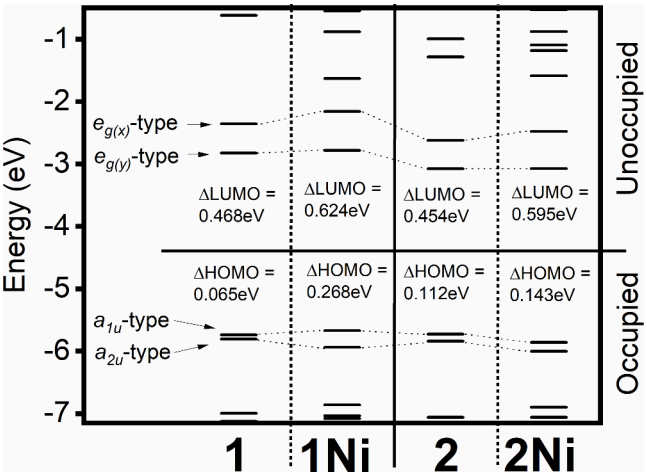

Figure 4. DFT-predicted energy-level diagram for the target compounds in the frontier MO region.

configuration that results in positive-to-negative sign sequences for the Q_x and Q_y bands (in ascending energy) of the major signals in the MCD spectrum and is typically only encountered in naturally occurring or synthetic hydroporphyrinoid systems. Thus, our DFT calculations correlate well with the experimental MCD spectra of **1**/**1Ni** and **2**/**2Ni** and further define both chromophores as typical chlorins.[18−21,45]

As mentioned above, the metalation of **1** and **2** results in the change of +--+ sequence for Q_x-Q_y-Soret(x)-Soret(y) bands in ascending energy to the +-+- sequence. Such a change is not new and was reported by Djerassi and co-workers for the metal-free/zinc pairs of chlorin, tetraphenylchlorin, and tetraphenylisobacteriochlorin.[45−47] Following his idea, such a change is indicative of an increased upon metalation |ΔHOMO − ΔLUMO| gap (or $|\Delta HOMO - \Delta LUMO|^2$ value, as summarized by Mack[14]). However, analysis of the |ΔHOMO − ΔLUMO| gap for **1** versus **1Ni** and **2** versus **2Ni** does not support this hypothesis (Figure 4). Indeed, while |ΔHOMO − ΔLUMO| increases between **2** and **2Ni**, it decreases between **1** and **1Ni**. As was speculated by us earlier for N-confused porphyrins,[48,49] the +-+- sequence was observed when the ΔLUMO was significantly increased upon metalation, and this is the case for **1Ni** and **2Ni**. Indeed, the DFT calculations predict that the ΔLUMO in metal-free **1** and **2** is ∼0.45−0.47 eV, while it increases to ∼0.60−0.62 eV upon metalation. Thus, it seems that the change of the ΔLUMO upon metalation plays a significant role in determination of the sign sequence in porphyrin analogues.

In order to determine the origins and band assignments of the major signals in the UV−vis spectra as well as to confirm the accuracy of the utilized computational method, TDDFT calculations were performed, with the relevant results presented in Figure 5 and Table 1.

The reasonable correlation between the theoretical and experimental data becomes obvious from inspection of Figure 5. In each chromophore investigated, the split or shouldered Soret band is accurately represented. The Q_x- and Q_y-band energies were also correctly predicted, and their intensities relative to the Soret bands nicely reproduce what is observed in the associated experimental spectra. In addition to the good agreement of the signal energies with experiment, the overall signal profiles were clearly simulated and reflect their experimental counterparts quite nicely. For compounds **1**/**1Ni** and **2**/**2Ni**, the Q_x- and Q_y-bands were found to be dominated by HOMO → LUMO excitations with a small portion (8−17%) of HOMO−1 → LUMO+1 transitions (Table 1). This is similar to several other chlorin- and bacteriochlorin-type modified porphyrins;[23] however, the excited state that is dominated by the HOMO−1 → LUMO single-electron excitation was also predicted in the Q-band region. Also, for all compounds, the Soret band, split or not, was determined to be dominated by an excited state containing prevalent HOMO → LUMO+1 single-electron excitations with small percentages of alternative transitions involving the four Gouterman's frontier orbitals included (Table 1). Thus, the most important features in the UV−vis spectra of **1**/**1Ni**

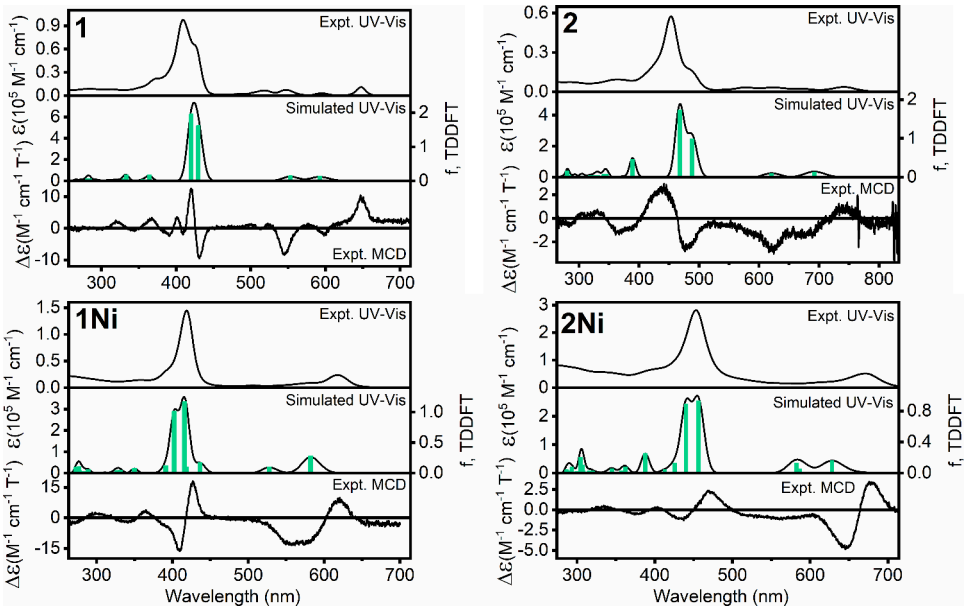

Figure 5. TDDFT-simulated UV−vis spectra of the compounds indicated (middle trace) in comparison to the experimental UV−vis spectra (upper trace) and the MCD spectra (both in CH_2Cl_2) (bottom trace).

https://doi.org/10.1021/acs.jpca.4c02803
J. Phys. Chem. A XXXX, XXX, XXX−XXX

Table 1. Select TDDFT-Predicted Signal Contributions for the Compounds Indicated

excited state	λ (nm)	E (cm^{-1})	oscillator strength, f	% contributions[a]
1				
1	593	16,873	0.1411	H→L (59%), H-1→L+1 (17%), H-1→L (17%), H→L+1 (6%)
2	553	18,081	0.1505	H-1→L (56%), H→L+1 (21%), H→L (18%), H-1→L+1 (5%)
3	430	23,277	1.6230	H-1→L+1 (47%), H→L+1 (26%), H→L (14%), H-1→L (11%)
4	420	23,789	1.9630	H→L+1 (46%), H-1→L+1 (29%), H-1→L (17%), H→L (8%)
5	364	27,464	0.1817	H-2→L (95%)
8	333	30,000	0.1769	H-3→L+1 (52%), H-5→L (38%)
1Ni				
5	582	17,168	0.2828	H→L (90%), H-1→L+1 (8%)
6	528	18,943	0.1010	H-1→L (74%), H→L+1 (25%)
7	436	22,914	0.1754	H→L+2 (81%), H→L+1 (13%), H-1→L (5%)
9	416	24,044	1.1700	H→L+1 (56%), H-1→L (18%), H→L+2 (16%), H-2→L (8%)
10	402	24,857	1.0130	H-1→L+1 (81%), H→L (8%), H-1→L+2 (6%)
11	391	25,575	0.1222	H-1→L+2 (75%), H-21→L+2 (10%), H-1→L+1 (8%)
37	277	36,126	0.1064	H→L+6 (51%), H-1→L+4 (15%), H→L+5 (13%), H-7→L+1 (4%)
2				
1	692	14,445	0.1341	H→L (83%), H-1→L+1 (14%)
3	488	20,478	0.9819	H-1→L+1 (77%), H→L (12%)
4	468	21,370	1.7250	H→L+1 (63%), H-1→L (31%)
5	389	25,679	0.4604	H-2→L (90%), H-1→L+1 (3%)
35	280	35,702	0.1587	H→L+5 (50%), H→L+4 (14%), H-1→L+4 (13%), H-1→L+6 (6%)
2Ni				
4	628	15,921	0.1621	H→L (80%), H-1→L+1 (12%)
6	582	17,172	0.1273	H-1→L (76%), H→L+1 (20%)
8	456	21,920	0.9301	H→L+1 (70%), H-1→L (19%), H→L+2 (6%)
9	440	22,712	0.8892	H-1→L+1 (80%), H→L (8%), H-4→L (5%)
10	426	23,483	0.1311	H-4→L (57%), H-5→L (33%), H-1→L+1 (5%)
12	388	25,790	0.2562	H→L+2 (83%), H-3→L (5%)
30	307	32,569	0.1057	H-1→L+4 (46%), H-1→L+3 (19%), H→L+4 (16%), H-15→L (5%),
31	305	32,812	0.2051	H-14→L (28%), H-5→L+1 (25%), H-4→L+1 (19%), H-16→L (12%), H-1→L+4 (6%)

[a]Only the contributions with >5% are shown.

and **2**/**2Ni** again can be rationalized within the boundaries of the Gouterman's four-orbital model.[4]

CONCLUSIONS

In conclusion, the electronic structures of porphyrinoids **1**/**1Ni** and **2**/**2Ni** were investigated by way of UV−vis and MCD spectroscopy as well as DFT and TDDFT computational methods. The UV−vis spectra possessed characteristics of typical chlorins. Accordingly, the MCD spectra of all compounds in the *Q*-band region featured the characteristic reversed sign sequence (i.e., positive-to-negative in ascending energy and HOMO−1 was represented by an a_{2u}-type orbital and HOMO by a_{1u}-type orbital), a situation generally found in β-alkylhydroporphyrinoids. The DFT-predicted ΔHOMO < ΔLUMO energy-level relationship in all cases is directly responsible for, and correlates well with, the reversed MCD sign sequences observed. Finally, the UV−vis spectra were accurately simulated using a TDDFT method, further validating the findings. Overall, these remarkable synthetic *meso*-aryl-substituted chlorin analogues were found to possess electronic structures comparable to those of naturally occurring hydroporphyrinoids. More importantly, the *seco*-type compounds **2** and **2Ni** have electronic structures and spectroscopic signatures that resemble those in chlorin-type porphyrin analogues. Thus, it is expected that the *seco*-porphyrins should have a ΔHOMO < ΔLUMO relationship. In addition, the presence of β-oxo groups and the drastic deviation from planarity of the chromophores **2**/**2Ni** red-shift their spectra significantly but do not affect their chlorin characteristics.

ASSOCIATED CONTENT

Supporting Information

The Supporting Information is available free of charge at https://pubs.acs.org/doi/10.1021/acs.jpca.4c02803.

Experimental part and additional DFT and TDDFT information (PDF)

AUTHOR INFORMATION

Corresponding Authors

Christian Brückner − *Department of Chemistry, University of Connecticut, Storrs, Connecticut 06269, United States;* orcid.org/0000-0002-1560-7345; Email: c.bruckner@uconn.edu

Victor N. Nemykin − *Department of Chemistry, University of Tennessee, Knoxville, Tennessee 37996, United States;* orcid.org/0000-0003-4345-0848; Email: vnemykin@utk.edu

Authors

Dustin E. Nevonen − *Department of Chemistry, University of Tennessee, Knoxville, Tennessee 37996, United States*

Adewole O. Atoyebi − *Department of Chemistry, University of Connecticut, Storrs, Connecticut 06269, United States;* orcid.org/0000-0002-9495-5072

Michael P. Luciano − *Department of Chemistry, University of Connecticut, Storrs, Connecticut 06269, United States;* orcid.org/0000-0002-1996-1587

Complete contact information is available at: https://pubs.acs.org/10.1021/acs.jpca.4c02803

Notes

The authors declare no competing financial interest.

ACKNOWLEDGMENTS

Generous support from the NSF, CHE-2153081 (to V.N.N.) and CHE-1800361 (to C.B.), the Minnesota Supercomputing Institute, and the University of Tennessee (both to V.N.N.) is greatly appreciated.

REFERENCES

(1) Battersby, A. R. Tetrapyrroles: the pigments of life. *Nat. Prod. Rep.* **2000**, *17*, 507−526.

(2) Dolphin, D., Ed.; *The Porphyrins*; Academic Press: New York, 1978; Vol. *1*.

(3) Dolphin, D., Ed.; *The Porphyrins*; Academic Press: New York, 1978; Vol. *2*.

(4) Lindsey, J. S. Synthesis of *meso*-substituted porphyrins. In *The Porphyrin Handbook*; Kadish, K. M.; Smith, K. M.; Guilard, R., Eds.; Academic Press: San Diego, 2000; Vol. *1*, pp 45−118.
(5) Taniguchi, M.; Lindsey, J. S. Synthetic Chlorins, Possible Surrogates for Chlorophylls, Prepared by Derivatization of Porphyrins. *Chem. Rev.* **2017**, *117*, 344−535.
(6) Shioi, Y. Large Scale Chlorophyll Preparations Using Simple Open-Column Chromatographic Methods. In *Chlorophylls and Bacteriochlorophylls*; Grimm, B.; Porra, R. J.; Rüdiger, W.; Scheer, H., Eds.; Springer: Dordrecht, NL, 2006; pp 123−131.
(7) Grinstein, M. Studies of Protoporphyrin: VII. Simple and Improved Method for the Preparation of Pure Protoporphyrin from Hemoglobin. *J. Biol. Chem.* **1947**, *167*, 515−519.
(8) Brückner, C.; Samankumara, L.; Ogikubo, J. Syntheses of Bacteriochlorins and Isobacteriochlorins. In *Handbook of Porphyrin Science*; Kadish, K. M.; Smith, K. M.; Guilard, R., Eds.; World Scientific:: River Edge, NY, 2012; Vol. *17*, pp 1−112.
(9) Borbas, K. E. Chlorins. In *Handbook of Porphyrin Science*; Kadish, K. M.; Smith, K. M.; Guilard, R., Eds.; World Scientific: River Edge, NY, 2016; Vol. *36*, pp 1−149.
(10) Gouterman, M. Spectra of Porphyrins. *J. Mol. Spectrosc.* **1961**, *6*, 138−163.
(11) Gouterman, M. Optical spectra and electronic structure of porphyrins and related rings. In *The Porphyrins*; Dolphin, D., Ed.; Academic Press: New York, 1978; Vol. *3*, pp 1−165.
(12) Michl, J. Electronic Structure of Aromatic π-Electron Systems as Reflected in Their MCD Spectra. *Pure Appl. Chem.* **1980**, *52*, 1549.
(13) Waluk, J.; Michl, J. Perimeter model and magnetic circular dichroism of porphyrin analogs. *J. Org. Chem.* **1991**, *56*, 2729−2735.
(14) Mack, J. Expanded, Contracted, and Isomeric Porphyrins: Theoretical Aspects. *Chem. Rev.* **2017**, *117*, 3444−3478.
(15) Doble, S.; Osinski, A. J.; Holland, S. M.; Fisher, J. M.; Geier, G. R.; Belosludov, R. V.; Ziegler, C. J.; Nemykin, V. N. Magnetic Circular Dichroism of Transition-Metal Complexes of Perfluorophenyl-N-Confused Porphyrins: Inverting Electronic Structure through a Proton. *J. Phys. Chem. A* **2017**, *121*, 3689−3698.
(16) Nevonen, D. E.; Wagner, J. C.; Brückner, C.; Ziegler, C. J.; Nemykin, V. N. Magnetic Circular Dichroism of Porphyrinoid Silver Complexes: Evidence of the Electronic Structure Inversion upon Protonation of the N-Confused Core. *J. Phys. Chem. Lett.* **2023**, *14*, 7382−7388.
(17) Kobayashi, N.; Muranaka, A.; Mack, J. Michl's Perimeter Model in MCD Spectroscopy. In *Circular Dichroism and Magnetic Circular Dichroism Spectroscopy for Organic Chemists*; The Royal Society of Chemistry: 2011.
(18) Keegan, J. D.; Stolzenberg, A. M.; Lu, Y. C.; Linder, R. E.; Barth, G.; Moscowitz, A.; Bunnenberg, E.; Djerassi, C. Magnetic circular dichroism studies. 61. Substituent-induced sign variation in the magnetic circular dichroism spectra of reduced porphyrins. 2. Perturbed molecular orbital analysis. *J. Am. Chem. Soc.* **1982**, *104*, 4317−4329.
(19) Keegan, J. D.; Stolzenberg, A. M.; Lu, Y. C.; Linder, R. E.; Barth, G.; Moscowitz, A.; Bunnenberg, E.; Djerassi, C. Magnetic circular dichroism studies. 60. Substituent-induced sign variation in the magnetic circular dichroism spectra of reduced porphyrins. 1. Spectra and band assignments. *J. Am. Chem. Soc.* **1982**, *104*, 4305−4317.
(20) Nonomura, Y.; Igarashi, S.; Yoshioka, N.; Inoue, H. Spectroscopic properties of chlorophylls and their derivatives. Influence of molecular structure on the electronic state. *Chem. Phys.* **1997**, *220*, 155−166.
(21) Umetsu, M.; Wang, Z.-Y.; Yoza, K.; Kobayashi, M.; Nozawa, T. Interaction of photosynthetic pigments with various organic solvents. 2. Application of magnetic circular dichroism to bacteriochlorophyll a and light-harvesting complex 1. *Biochim. Biophys. Acta* **2000**, *1457*, 106−117.
(22) Rhoda, H. M.; Akhigbe, J.; Ogikubo, J.; Sabin, J. R.; Ziegler, C. J.; Brückner, C.; Nemykin, V. N. Magnetic Circular Dichroism Spectroscopy of *meso*-Tetraphenylporphyrin-Derived Hydroporphyrins and Pyrrole-Modified Porphyrins. *J. Phys. Chem. A* **2016**, *120*, 5805−5815.
(23) Brückner, C.; Chaudhri, N.; Nevonen, D. E.; Bhattacharya, S.; Graf, A.; Kaesmann, E.; Li, R.; Guberman-Pfeffer, M. J.; Mani, T.; Nimthong-Roldán, A.; Zeller, M.; et al. Structural and Photophysical Characterization of All Five Constitutional Isomers of the Octaethyl-β,β′-dioxo-bacterio- and -isobacteriochlorin Series. *Chem. − Eur. J.* **2021**, *27*, 16189−16203.
(24) Zhang, A.; Stillman, M. J. Exploring function activated chlorins using magnetic circular dichroism spectroscopy and density functional theory methods: design of a chlorin with a remarkably intense, red Q band. *Phys. Chem. Chem. Phys.* **2018**, *20*, 12470−12482.
(25) Yu, Y.; Furuyama, T.; Tang, J.; Wu, Z.-Y.; Chen, J.-Z.; Kobayashi, N.; Zhang, J.-L. Stable iso-bacteriochlorin mimics from porpholactone: effect of a β-oxazolone moiety on the frontier π-molecular orbitals. *Inorg. Chem. Frontiers* **2015**, *2*, 671−677.
(26) Menezes, J. C. J. M. D. S.; Faustino, M. A. F.; de Oliveira, K. T.; Uliana, M. P.; Ferreira, V. F.; Hackbarth, S.; Roeder, B.; Teixeira-Tasso, T.; Furuyama, T.; Kobayashi, N.; et al. Synthesis of New Chlorin e6 Trimethyl and Protoporphyrin IX Dimethyl Ester Derivatives and Their Photophysical and Electrochemical Characterizations. *Chem. − Eur. J.* **2014**, *20*, 13644−13655.
(27) Luciano, M.; Tardie, W.; Zeller, M.; Brückner, C. Supersizing Pyrrole-modified Porphyrins by Reversal of the 'Breaking and Mending' Strategy. *Chem. Commun.* **2016**, *52*, 10133−10136.
(28) Luciano, M. P.; Atoyebi, A. O.; Tardie, W.; Zeller, M.; Brückner, C. Pyrrole-Modified Porphyrins Containing Eight-Membered Heterocycles Using a Reversal of the "Breaking and Mending" Strategy. *J. Org. Chem.* **2020**, *85*, 15273−15286.
(29) Crossley, M. J.; Govenlock, L. J.; Prashar, J. K. Synthesis of porphyrin-2,3,12,13- and −2,3,7,8-tetraones: building blocks for the synthesis of extended porphyrin arrays. *J. Chem. Soc., Chem. Commun.* **1995**, 2379−2380.
(30) Brückner, C.; McCarthy, J. R.; Daniell, H. W.; Pendon, Z. D.; Ilagan, R. P.; Francis, T. M.; Ren, L.; Birge, R. R.; Frank, H. A. A spectroscopic and computational study of the singlet and triplet excited states of synthetic ß-functionalized chlorins. *Chem. Phys.* **2003**, *294*, 285−303.
(31) Taniguchi, M.; Kim, H.-J.; Ra, D.; Schwartz, J. K.; Kirmaier, C.; Hindin, E.; Diers, J. R.; Prathapan, S.; Bocian, D. F.; Holten, D.; Lindsey, J. S. Synthesis and Electronic Properties of Regioisomerically Pure Oxochlorins. *J. Org. Chem.* **2002**, *67*, 7329−7342.
(32) Taniguchi, M.; Ra, D.; Kirmaier, C.; Hindin, E.; Schwartz, J. K.; Diers, J. R.; Knox, R. S.; Bocian, D. F.; Lindsey, J. S.; Holten, D. Comparison of Excited-State Energy Transfer in Arrays of Hydroporphyrins (Chlorins, Oxochlorins) versus Porphyrins: Rates, Mechanisms, and Design Criteria. *J. Am. Chem. Soc.* **2003**, *125*, 13461−13470.
(33) Liu, M.; Chen, C.-Y.; Hood, D.; Taniguchi, M.; Diers, J. R.; Bocian, D. F.; Holten, D.; Lindsey, J. S. Synthesis, photophysics and electronic structure of oxobacteriochlorins. *New J. Chem.* **2017**, *41*, 3732−3744.
(34) Hood, D.; Niedzwiedzki, D. M.; Zhang, R.; Zhang, Y.; Dai, J.; Miller, E. S.; Bocian, D. F.; Williams, P. G.; Lindsey, J. S.; Holten, D. Photophysical characterization of tolyporphin A, anaturally occurring dioxobacteriochlorin, and synthetic oxobacteriochlorin analogues. *Photochem. Photobiol.* **2017**, *93*, 1204−1215.
(35) Chaudhri, N.; Guberman-Pfeffer, M. J.; Li, R.; Zeller, M.; Brückner, C. β-Trioxopyrrocorphins: Pyrrocorphins of Graded Aromaticity. *Chem. Sci.* **2021**, *12*, 12292−12301.
(36) Brückner, C. The Breaking and Mending of *meso*-Tetraarylporphyrins: Transmuting the Pyrrolic Building Blocks. *Acc. Chem. Res.* **2016**, *49*, 1080−1092.
(37) Luciano, M. P.; Akhigbe, J.; Ding, J.; Thuita, D.; Hamchand, R.; Zeller, M.; Brückner, C. An Alternate Route of Transforming meso-Tetraarylporphyrins to Porpholactams, and Their Conversion to Amine-Functionalized Imidazoloporphyrins. *J. Org. Chem.* **2018**, *83*, 9619−9630.

https://doi.org/10.1021/acs.jpca.4c02803
J. Phys. Chem. A XXXX, XXX, XXX−XXX

(38) Hewage, N.; Daddario, P.; Lau, K. S. F.; Guberman-Pfeffer, M. J.; Gascón, J. A.; Zeller, M.; Lee, C. O.; Khalil, G. E.; Gouterman, M.; Brückner, C. Bacterio- and Isobacteriodilactones by Stepwise or Direct Oxidations of *meso*-Tetrakis(pentafluorophenyl)porphyrin. *J. Org. Chem.* **2019**, *84*, 239−256.
(39) Frisch, M. J.; Trucks, G. W.; Schlegel, H. B.; Scuseria, G. E.; Robb, M. A.; Cheeseman, J. R.; Scalmani, G.; Barone, V.; Petersson, G. A.; Nakatsuji, H.; Li, X. et al. *Gaussian 16, Revision B.01*; Gaussian, Inc.: Wallingford CT, 2016. For full citation, see Supporting Information.
(40) Zhao, Y.; Truhlar, D. G. The M06 suite of density functionals for main group thermochemistry, thermochemical kinetics, noncovalent interactions, excited states, and transition elements: two new functionals and systematic testing of four M06-class functionals and 12 other functionals. *Theor. Chem. Acc.* **2008**, *120*, 215−241.
(41) Wachters, A. J. H. Gaussian Basis Set for Molecular Wavefunctions Containing Third-Row Atoms. *J. Chem. Phys.* **1970**, *52*, 1033−1036.
(42) McLean, A. D.; Chandler, G. S. Contracted Gaussian-Basis Sets for Molecular Calculations. 1. 2nd Row Atoms, Z = 11−18. *J. Chem. Phys.* **1980**, *72*, 5639−5648.
(43) Tomasi, J.; Mennucci, B.; Cammi, R. Quantum Mechanical Continuum Solvation Models. *Chem. Rev.* **2005**, *105*, 2999−3093.
(44) Tenderholt, A. L. *QMForge, version 2.1*; Stanford University: Stanford, CA, 2011. https://qmforge.net/.
(45) Keegan, J. D.; Stolzenberg, A. M.; Lu, Y. C.; Linder, R. E.; Barth, G.; Moscowitz, A.; Bunnenberg, E.; Djerassi, C. Magnetic circular dichroism studies. 60. Substituent-induced sign variation in the magnetic circular dichroism spectra of reduced porphyrins. 1. Spectra and band assignments. *J. Am. Chem. Soc.* **1982**, *104*, 4305−4317.
(46) Keegan, J. D.; Stolzenberg, A. M.; Lu, Y.-C.; Linder, R. E.; Barth, G.; Moscowitz, A.; Bunnenberg, E.; Djerassi, C. Magnetic circular dichroism studies. 61. Substituent-induced sign variation in the magnetic circular dichroism spectra of reduced porphyrins. 2. Perturbed molecular orbital analysis. *J. Am. Chem. Soc.* **1982**, *104*, 4317−4329.
(47) Keegan, J. D.; Stolzenberg, A. M.; Lu, Y.-C.; Linder, R. E.; Barth, G.; Moscowitz, A.; Bunnenberg, E.; Djerassi, C. Magnetic circular dichroism studies. 59. Substituent-induced sign variation in the magnetic circular dichroism spectra of chlorins. *J. Am. Chem. Soc.* **1981**, *103*, 3201−3203.
(48) Ziegler, C. J.; Erickson, N. R.; Dahlby, M. R.; Nemykin, V. N. Magnetic Circular Dichroism Spectroscopy of N-Confused Porphyrin and Its Ionized Forms. *J. Phys. Chem. A* **2013**, *117*, 11499−11508.
(49) Sripothongnak, S.; Ziegler, C. J.; Dahlby, M. R.; Nemykin, V. N. Controllable and reversible inversion of the electronic structure in nickel N-confused porphyrin: a case when MCD matters. *Inorg. Chem.* **2011**, *50*, 6902−6909.

https://doi.org/10.1021/acs.jpca.4c02803
J. Phys. Chem. A XXXX, XXX, XXX−XXX